Selective epitaxial growth of Ge nanodots with ultra-thin porous alumina membrane

Wenbo Zhan (詹文博)[1], Yourui Huangfu (皇甫幼睿)[1], Xu Fang (方 旭)[1], Xia Hong (洪 霞)[1], Liang Xia (夏 亮)[1], Xiongbin Guo (郭雄彬)[2], and Hui Ye (叶 辉)[1*]

[1]*State Key Laboratory of Modern Optical Instrumentation, Zhejiang University, Hangzhou 310027, China*

[2]*Research Institute of Energy and Nuclear Technology Application of Zhejiang Province, Hangzhou 310012, China*

**Corresponding author: huiye@zju.edu.cn*

Received December 20, 2012; accepted January 15, 2013; posted online April 19, 2013

We demonstrate that ultra-thin porous alumina membrane (PAM) is suitable for controlling of both size and site of Ge nanodots on Si substrates. Ge nanodots are grown on Si substrates with PAM as a template at different temperatures with molecular beam epitaxy (MBE) method. Ordered Ge nanodot arrays with uniform size and high density are obtained at 400 and 500 °C. Spatial frequency spectrums transformed from scanning electron microscopy images through fast Fourier transform are utilized to analyze surface morphologies of Ge nanodots. The long-range well-ordered Ge nanodot arrays form a duplication of PAM at 400 °C while the hexagonal packed Ge nanodot arrays are complementary with PAM at 500 °C.

OCIS codes: 160.4236, 100.2000, 130.5990.

doi: 10.3788/COL201311.S10206.

In recent decades, Si-based Ge quantum dots (QDs) are highly expected in various electronic and optoelectronic applications such as infrared photodetectors[1], single-electron devices[2], light emitting diode or laser[3], nonlinear optical devices[4], and quantum computers[5] due to their optoelectronic potential. In order to well realize all these applications and optimize their performances, the characteristics of Ge QDs, including size distribution, spatial site, shape, and density, should be successfully controlled by existing growth techniques. However, Ge QDs obtained by conventional Stranski-Krastanov (S-K) mode have always large size and site distributions that may contribute a negative impact to device performances. For the purpose of achievement of ordered uniform Ge QDs and their quantum effects, considerable attention has turned towards growing controllable Ge QDs using well-patterned Si substrates. A lot of patterning techniques such as electron beam lithography[6], focused ion beam (FIB)[7], extreme ultraviolet interference lithography (EUV-IL)[8], and holographic lithography[9] have been widely used. But all of these techniques are complex in progress and expensive as well. A kind of porous alumina membrane (PAM) with densely hexagonal packed and straight nanopores, acting as a nano-patterned template without lithography, can be a cost-effective alternative approach to formation of well-ordered Ge QD arrays with high density, uniform size, and hexagonal spatial distribution.

In this letter, large areas of aligned arrays of Ge nanodots with uniform size distribution are grown on Si substrates with PAM by molecular beam epitaxy (MBE) method. Our results shows that the diffusion of Ge adatoms is restricted by PAM at 400 and 500 °C resulting in long-range ordered nano-structures.

An ultra-thin free-standing PAM that would be transferred to Si substrate later was fabricated through a typical two-step electrochemical procedure with high-purity (99.999%) aluminum foils. After two-step anodization, removing unanodized aluminum in a mixture of $CuSO_4$/HCl and dissolving barrier layer in 5 wt.-% H_3PO_4[10], the free-standing PAM remained to be attached to Si substrate via van der Waals force. The PAM we used was obtained with average pore diameter of 80 nm, average interpore distance around 100 nm, thickness of 200 nm, and pore density as high as 10^{10} cm^{-2}. To protect the PAM, there was no chemical treatment after PAM transferred to Si substrate, while the Si substrate was chemically cleaned with standard root cause analysis (RCA) process before. During the deposition in the MBE process, Ge nanodots were grown at different substrate temperatures of 400, 500, and 600 °C. The flux rate was about 0.005 nm/min and the final coverage of Ge was 20 nm. After growth, the surface morphologies of deposited Ge nanodots were observed by a scanning electron microscopy (SEM) (Zeiss Ultra-55).

Figure 1 shows the SEM image of the sample grown at 600 °C. In Fig. 1, the PAM attached to the Si substrate cannot withstand such a high temperature, resulting in fracture. Consequently, deposited Ge accumulates to nanodots with random spatial sites and broad size distribution due to PAM losing its limitation. Obviously, PAM does not work at 600 °C.

To protect PAM from high temperature, a medium temperature sample is prepared at 500 °C, which is shown in Fig. 2(a) after removing PAM with a NaOH

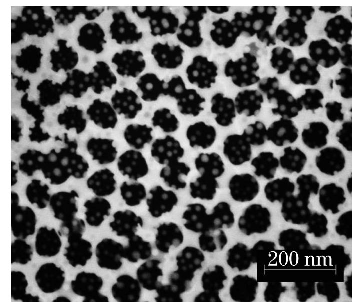

Fig. 1. SEM image of the Ge nanodots grown at 600 °C.

 © 2013 Chinese Optics Letters

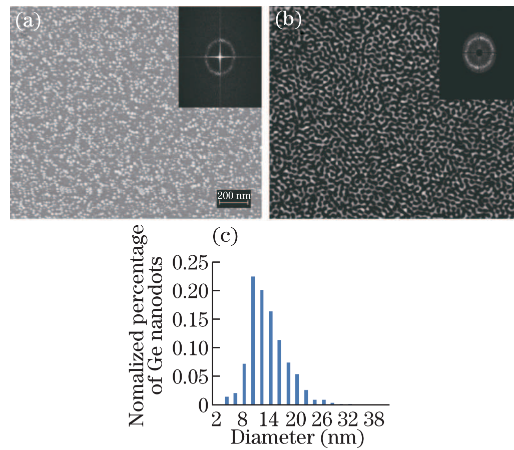

Fig. 2. (a) SEM image of the Ge nanodots after removing PAM at 500 °C and its FFT spatial frequency spectrum (inset); (b) spatial frequency spectrum after filtering (inset) and its regenerated image through inverse FFT; (c) size distribution of Ge nanodots grown at 500 °C with changes in diameter.

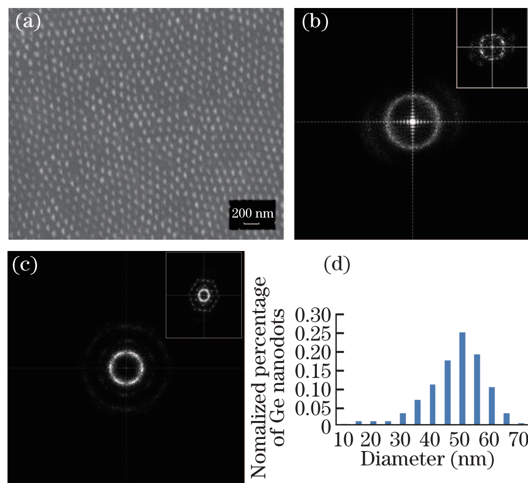

Fig. 3. (a) SEM image of Ge nanodots grown at 400 °C; (b) FFT spatial frequency spectrum of a large area and a small area (inset) of Ge nanodots grown at 400 °C; (c) FFT spatial frequency spectrum of a large area and a small area (inset) of PAM; (d) size distribution of Ge nanodots grown at 400 °C with changes in diameter.

solution. Despite the disorder of Ge nanodots appeared in a small area, an indistinct hexagonal netlike structure looms in a large range, just like a copy of PAM, is confirmed by the frequency spectrum after fast Fourier transform (FFT) shown in the inset of Fig. 2(a). After filtering noise frequency in the two orthogonal directions and part of high-frequency resulting from some neglected tiny particles, the spatial frequency spectrum of the Ge nanodot structures is revealed in the inset of Fig. 2(b). Next the spectrum is turned to another plan-view micrograph of the medium temperature sample shown in Fig. 2(b). Although many breaks retained there, a mostly complete honeycomb-like structure reappears clearly. It is much more strongly turned out that the morphology of Ge nanodots in a large area seems like a duplication of PAM. The main purpose of introduction of PAM is to limit the diffusion of Ge adatoms and restrict the nucleate sites of Ge nanodots. However, at growth temperature of 500 °C that PAM fully remains, considerable amount of Ge adatoms are still able to migrate to the borders of separated areas in the bottom of pores of PAM respectively, so that the surface energy may keep lowest. Ge adatoms in the edge areas always have much more close neighbors than any other positions, because surface energy makes adatoms migrate to somewhere they have the most neighbors around them[11]. But, there are not all Ge adatoms moving to the borders as the growth temperature is not so high that the migration lengths of all Ge adatoms are large enough. Figure 2(c) shows the statistic size distribution of Ge nanodots of the medium temperature sample. The x axis is diameter of Ge nanodots and the y axis stands for normalized percentage. Instead of a bimodal distribution found in conventional S-K growth mode, only a single peak around 10 nm appears in the figure. It results from the coalescence of Ge nanodots from different pore cells blocked by PAM, so that there are no relatively big Ge nanodots. Obviously, the density of Ge nanodots here is several times of the one of the pores of PAM.

The surface morphology of the low temperature sample grown at 400 °C is shown in Fig. 3(a). As the growth temperature decreases, the diffusion of Ge adatoms is further limited. Tending to stay fixed or migrate in a quite small range rather than nucleating in the borders, Ge adatoms assemble into only one nanodot per PAM pore, just emerged in Fig. 3(a). Following with the same transform treatment about spatial frequency spectrum as the medium temperature sample, the spatial frequency spectrum of a large area of the low temperature sample is shown in Fig. 3(b), while the one of a small area is revealed in the inset of Fig. 3(b). As a comparison, the spatial frequency spectrums of large and small areas of PAM template are also shown in Fig. 3(c) and the inset of Fig. 3(c), respectively. Orthogonal lines in Figs. 3(b) and (c) stand for some noise resulting from irregular nanostructures, signal boost and process of SEM capture. For the large area spectrum of PAM, there are clearly three rings. The brightest one is the 1st stripe of FFT containing main information of spatial distribution of Ge nanodots with low-frequency, which may dominate the pattern of Ge nanodots arrays. There are six symmetrical brighter arcs composed of the the 1st stripe because of the hexagonal packed pores of PAM. It is confirmed by the small area spectrum, where all stripes are hexagons. For the low temperature sample, whose FFT patterns are not so bright as those of PAM, two FFT stripes still appear. Similar with the spatial frequency spectrums of PAM, the 1st ring indicates ordered distribution of Ge nanodots, and the one in the inset proves the hexagonal shape as well. So, passing through the PAM, Ge accumulates to nanodots in the bottom of the PAM pores. What is more, long-range ordered, hexagonal packed, and triangular pyramid Ge nanodots with almost uniform size are obviously complementary to PAM. The reason of triangular pyramid shape of Ge nanodots is attributed to shadowing effect due to the introduction of PAM. The shadowing effect is composed of two main reasons: the aspect ratio of PAM and the angle between evaporator of our MBE system and vertical direction. The aspect ratio of PAM we used is about 1:3. Additionally, there

is an angle around 15° between the evaporator and vertical direction. As a consequence, the equivalent aspect ratio may be 1:6 here, leading to triangular shape of Ge nanodots[12]. Also, the statistic size distribution of Ge nanodots of the low temperature sample is plotted in Fig. 3(d). A single main peak around 50 nm in diameter is found, much bigger than the mean diameter of Ge nanodots of the medium temperature sample. The deposited Ge dispersing to forming numerous nanodots in the edges of separated cells for the medium temperature sample, now coalesces into only a huge nanodot in every cell. The density of Ge nanodots reaching 10^{10} cm^{-2} is equal to the one of PAM pores.

As mentioned above, PAM confines diffusion of Ge adatoms by separated straight pores resulting in the migration length losing its dependence on temperature. Generally, the higher the growth temperature is, the larger the migration length of Ge adatoms is. However, because of PAM, the migration length is never larger than diameter of pores of PAM despite of growth temperature increasing, while PAM is not broken. Only in the situation where the temperature is lower than the one corresponding migration length is smaller than the diameter of PAM pores, the migration length will vary with changes in temperature. So, it becomes easier to find the optimal growth temperature here. Confinement of diffusion also leads to other two advantages. Firstly, sites of Ge nanodots are restricted in the narrow areas in the bottom of nanopores, forming long-range ordered arrays no matter where Ge nanodots nucleate, in the borders or not. On the other hand, there is certainly a narrow size distribution of Ge nanodots owing to similar deposited amount of Ge from different nanopores.

In conclusion, we investigate the surface morphologies of Ge nanodots grown at different temperatures of 400, 500 and 600 °C by MBE method. The diffusion of Ge is limited by PAM at 400 and 500 °C, that PAM is not broken. As a consequence, long-range ordered spatial distributions of Ge nanodots are observed, confirmed, and analyzed by comparison among different FFT spatial frequency spectrums. Uniform Ge nanodots with narrow size distributions and high densities are found in samples at 400 and 500 °C.

This work was supported by the Natural Science Foundation of Zhejiang Province (No. LZ12F04002) and the Science and Technology Project of Zhejiang Province (No. 2011F20021).

References

1. S. Tong, F. Liu, A. Khitun, K. L. Wang, and J. L. Liu, J. Appl. Phys. **96,** 773 (2004).
2. P. W. Li, W. M. Liao, David M. T. Kuo, S. W. Lin, P. S. Chen, S. C. Lu, and M. J. Tsai, Appl. Phys. Lett. **85,** 1532 (2004).
3. J. S. Xia, K. Nemoto, Y. Ikegami, Y. Shiraki, and N. Usami, Appl. Phys. Lett. **91,** 011104 (2007).
4. P.D. Tougaw, C. S. Lent, and W. Porod, J. Appl. Phys. **74,** 3558 (1993).
5. B. E. Kane, Nature **393,** 133 (1998).
6. G. Chen, G. Vastola, H. Lichtenberger, D. Pachinger, G. Bauer, W. Jantsch, F. Schäffler, and L. Miglio, Appl. Phys. Lett. **92,** 113106 (2008).
7. A. Portavoce, M. Kammler, R. Hull, M. C. Reuter, and F. M. Ross, Nanotechnology **17,** 4451 (2006).
8. D. Grützmacher, T. Fromherz, C. Dais, J. Stangl, E. Müller, Y. Ekinci, H. H. Solak, H. Sigg, R. T. Lechner, E. Wintersberger, S. Birner, V. Holý, and G. Bauer, Nano Lett. **7,** 3150 (2007).
9. Z. Y. Zhong, A. Halilovic, M. Mühiberger, F. Schäffler, and G. Bauer, Appl. Phys. Lett. **82,** 445 (2003).
10. G. Q. Ding, M. J. Zheng, W. L. Xu, and W. Z. Shen, Nanotechnology **16,** 1285 (2005).
11. E. Kasper, *Properties of Strained and Relaxed Silicon Germanium* (NDIP, Beijing, 2002).
12. Y. Lei and W. K. Chim, Chem. Mater. **17,** 580 (2005).